Theoretical calculation of the acoustic force on a patterned silicon wafer during megasonic cleaning

P. A. Deymier[a)]
Department of Materials Science and Engineering, University of Arizona, Tucson, Arizona 85721

A. Khelif, B. Djafari-Rouhani, and J. O. Vasseur
Laboratoire de Dynamique et Structure des Matériaux Moléculaires, UPRESA CNRS 8024, UFR de Physique, Université des Sciences et Technologies de Lille, 59655 Villeneuve d'Ascq, France

S. Raghavan
Department of Materials Science and Engineering, University of Arizona, Tucson, Arizona 85721

(Received 18 February 1999; accepted for publication 25 May 2000)

We have calculated, theoretically, the acoustic pressure field around a linear pattern on a silicon wafer immersed in water subjected to a megasonic beam. The method of calculation is based on a Green's function formalism. The acoustic force applied on the pattern by the pressure field is determined as a function of frequency and the angle the incident megasonic beam makes with the wafer surface. The calculation is applied to two types of features that may be encountered in megasonic cleaning of integrated circuits prior to packaging, namely a micron-size silicon ridge and a metal wire (tens to hundreds of microns in diameter) bonded on a silicon substrate. The calculated acoustic shear stress is found to be orders of magnitude smaller than the shear strength of the features. © *2000 American Institute of Physics.* [S0021-8979(00)03017-6]

I. INTRODUCTION

Megasonic waves have been extensively used to remove contaminant particles from silicon wafers during manufacturing of semiconductor devices. In this process, planar silicon wafers are immersed in a water-based fluid solution and subjected to a beam of sonic energy with frequency in the range from 600 kHz to 1 MHz. There has been interest in cleaning nonplanar patterned wafers (for instance vias cleaning) with megasonic waves. However, little is known about the potential damaging effects that the acoustic energy may have on the integrity of the pattern. Several physical processes associated with acoustic cleaning such as microcavitation, acoustic streaming, and acoustic pressure force may have a detrimental impact on the patterned wafers.

Microcavitation is produced by the pressure variations in sound waves moving through the liquid. Cavitation bubbles are formed by the low-pressure component of the acoustic wave. A cavity implodes when the walls can no longer sustain the compressive forces thus transferring energy from the cavity to the surrounding medium. Cavitation is ubiquitous in ultrasonic cleaning systems. In ultrasonic cleaning (with frequencies in the range from 17 to about 100 kHz), cavitation is known to damage the wafer surface, and ultrasounds are typically avoided in wafer processing. Megasonic cleaning is similar to ultrasonic cleaning but it uses higher frequencies on the order from 600 kHz to 1 MHz. It had been believed that the short time between megasonic pulses on the order of 1–1.25 μs, does not promote the formation of cavities and may therefore lead to less wafer damage.[1] More recently, cavitation was detected in a megasonic tank by sonoluminescence.[2] These experimental measurements however indicate that the maximum cavitation intensity occurs near the water surface of the megasonic tank.

Acoustic streaming is a time-independent fluid motion generated by a sound field. There are several types of acoustic streaming classified in terms of scale, namely Eckart's quartz-wind-like streaming,[3] Schlicting streaming in boundary layers near surfaces of obstacles,[4] and microstreaming near secondary sound sources such as oscillating bubbles or vibrating particles on surfaces.[5] Pattern features at the surface of the wafer may be damaged by the fluid flow.

Finally, pressure gradients near features on a wafer may also exert damaging forces. The megasonic waves can be visualized as pressure variations propagating into the fluid at the speed of sound. When a sonic wave passes tangentially over the wafer, the pressure gradient in that wave may be expected to exert a force on any feature that may be present on the wafer. If the wavelength is comparable to the feature size scattering may occur, and consequently, the acoustic pressure on the feature may depend not only on the incident wave but also on the scattered wave. Finally, the oscillatory nature of the acoustic field may be responsible for fatigue damage.

Experimental studies on the effect of megasonic cleaning on wafer damage will therefore be clouded by the superposition of the processes briefly discussed above. An experimental investigation of megasonic cleaning is further complicated by the very small spatial and temporal scales at which some of these processes take place. We have therefore elected to undertake a systematic theoretical investigation of these various processes aimed at identifying which one may be detrimental to the integrity of patterned wafers during cleaning. It is the purpose of this article to shed light on the

[a)]Electronic mail: deymier@oxygen.mse.arizona.edu

potential damage the oscillatory acoustic pressure field of the megasonic wave may inflict on a patterned wafer. For this, we analyze the interaction between an incident acoustic wave and a silicon substrate supporting a raised linear feature. A methodology based on Green's functions has been developed to calculate the acoustic field around the feature (or surface defect). The acoustic pressure field is then integrated over the surface of the defect to calculate the acoustic force on the defect and, in particular, its components along and perpendicular to the wafer surface. We show that the acoustic force varies with the angle of incidence of the sonic beam as well as the frequency of the sound wave. Only the component of the acoustic force tangential to the surface of the wafer exhibits a strong dependence on the angle of incidence and frequency in the range of frequencies used in megasonic cleaning.

We apply the model to the calculation of the acoustic force on two types of raised linear features with significantly different sizes that may be encountered in megasonic cleaning of integrated circuits. The first feature is a micron-size silicon ridge on the silicon substrate while the second one consists of a thin metallic wire bonded on a silicon wafer with diameter in the tens to hundreds of micron. A comparison between the calculated acoustic stress in the silicon linear defect and the adhesion strength of raised silicon features on silicon wafers suggests that the acoustic force cannot lead to the damage of silicon features on silicon patterned wafers. Similar conclusions are drawn for the effect of a megasonic wave on metallic wires bonded on a substrate. The acoustic shear stress can be larger in this case (in particular for large diameter wires) than for the micron-size silicon ridge. The maximum shear strength of bonded metal wires exceeds the acoustic stress by more than one order of magnitude and damage of the bonded wires is quite improbable. The acoustic wave may, however, have a damaging effect only for poor quality bonds with very low shear strength.

This article is organized as follows: The model is presented in Sec. II. Section III includes the application of the model to the calculation of an acoustic shear stress on the two types of raised linear features. The calculated acoustic shear stress is compared to available data for shear strength of the materials considered. Finally, conclusions are drawn in Sec. IV concerning the safety of cleaning patterned wafers with megasonic waves.

II. METHOD OF CALCULATION AND RESULTS

The geometry of the inhomogeneous solid/fluid interface is sketched in Fig. 1. The solid region is composed of a raised feature or linear defect ''a'' located on the planar surface of the substrate. The substrate fills the half space $x_3 < 0$ and the axis of the defect is oriented parallel to the x_2 direction of the Cartesian coordinate system $(Ox_1x_2x_3)$. The raised feature may then be visualized as an infinitely long ridge in the x_2 direction. We have assumed that the defect cross section in the (x_1,x_3) plane has a parabolic shape defined by

$$f(x_1) = a\left[1 - \left(\frac{x_1}{R}\right)^2\right] \quad \text{for} \quad x_1 \in [-R,R].$$

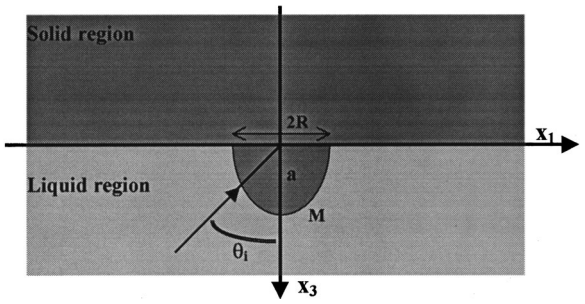

FIG. 1. Schematic representation of the inhomogeneous interface solid/fluid. The axis of the linear defect a is along x_2 (not represented) and orthogonal to x_1, x_3.

The height of the parabola is taken to be $a = 2R$. Raised features on the wafer do not typically exhibit parabolic cross sections; however, we have made this choice for the sake of mathematical practicality.

In this article, we assume that the solid is made up of an infinitely rigid medium. The assumption of infinite rigidity means that the modulus of compressibility of the solid is infinite. However, in order to keep the usual speed of sound finite, it is necessary to assume that the density of the solid is also infinite. This hypothesis, which is rather well justified for many solids immersed in water, implies that the vibrations do not penetrate into the solid region, and hence the propagation is confined in the liquid. In order to verify this hypothesis we have calculated the square of the coefficient of reflection of a plane wave at a silicon/water interface when surface waves and attenuation are not considered. For this calculation we have used expressions for the partition of energy between the incident, reflected, and refracted portions of a sonic wave given in Refs. 6 and 7. We also use the following data: a silicon density of 2.33×10^3 kg/m^3, a density of water of 10^3 kg/m^3, longitudinal speed of sound in water of 1500 m/s, and transverse and longitudinal speeds of sound in silicon of 5843 m/s and 8433 m/s, respectively. The calculated coefficient of reflection as a function of incident angle is reported in Fig. 2. For most angles of incidence, the coefficient of reflection may be seen to take the value one indi-

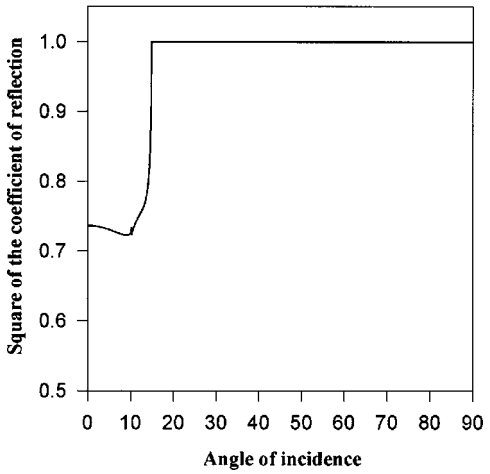

FIG. 2. Square of the coefficient of reflection of a silicon/water planar interface as a function of incidence angle.

cating that the approximation of rigidity of the solid is valid. Below an incidence angle of approximately 15° only about 75% of the incident wave is reflected in the fluid with the remainder transmitted through the solid. Under these conditions the solid may not be assumed to be rigid and any such approximation will lead to a cruder estimation of the true acoustic pressure in the fluid. Since 75% of the wave is still reflected, the calculated pressure is likely to remain a reasonable estimate of the true pressure.

We now set up the model for the raised linear feature on a silicon substrate immersed in water. As stated previously, the feature and the substrate are now treated as rigid solids. Because of the low viscosity of water and for the sake of mathematical tractability of this problem, we will assume that the fluid is nonviscous. This assumption is justified for the following reasons. The viscosity of a fluid has several effects on the sound field near a solid/fluid interface. First, continuity of the displacement at the interface between an elastic solid and a viscous fluid must be satisfied even for vanishingly small viscosities. Therefore, despite the small but finite viscosity of water (0.001 Pa s), we will seek a solution for the acoustic field that satisfies the condition of continuity of displacement at the interface. Second, a viscous fluid can sustain transverse waves, however, for the small viscosity of water, the longitudinal component of the wave dominates and constitutes the main contribution to the displacement field. Third, the displacement of an acoustic wave propagating in a viscous medium is attenuated. This attenuation may be ignored for (a) fluids with small viscosities and (b) spatial distributions of the acoustic field over small length scales (such as that of the linear defects considered in this study). Finally, viscosity leads to time-independent second order effects such as acoustic streaming. Acoustic streaming may be treated as a nonlinear correction to the linear (first order) acoustic field. Since the objective of the present article is on the calculation of the impact of the time-dependent (first order) acoustic pressure field on patterned wafers, we focus here on solving the linear equation of motion for elastic media. Under the assumption of a nonviscous liquid, only longitudinal waves are allowed and they obey the following equation of motion:

$$\rho(r)\frac{\partial^2 u}{\partial t^2}=\nabla(\rho(r)c_l^2(r)\nabla u), \tag{1}$$

where $\rho(r)$ is the mass density, $c_l(r)$ is the longitudinal speed of sound, and u represents the elastic displacement field. Since the solid is rigid, that is $u=0$ everywhere within the solid, the boundary condition at the solid–liquid interface should also express the vanishing of the elastic displacement u in the direction normal to the interface. This condition satisfies the continuity of the displacement at the fluid/solid interface.

In the case of irrotational motion of the fluid, $\nabla\times(\rho u)=0$ and it is possible to define a scalar potential $\phi(r,t)$ such that $\rho\varpi^2 u=\nabla\phi$. Then Eq. (1) may be rewritten as

$$\chi\frac{\partial^2\phi}{\partial t^2}=\nabla(\rho^{-1}\nabla\phi), \tag{2}$$

where $\chi=(\rho c_l^2)^{-1}$ is the compressibility of the liquid. Assuming that the fluid undergoes harmonic motion with a time-dependence $e^{-i\varpi t}$, Eq. (2) takes the form

$$\frac{1}{\rho}\left(\frac{\partial}{\partial x_1^2}+\frac{\partial}{\partial x_3^2}+\frac{\omega^2}{c_l^2}\right)\phi(x_1,x_3)=0. \tag{3}$$

In the problem at hand, we must therefore solve Eq. (3) for the liquid motion subject to the boundary condition $\nabla\phi=0$ in the direction normal to the solid–liquid interface. For this we employ a method based on Green's functions. Equation (3) may be written in the form, $H\phi=0$, where the differential operator H is defined as

$$H=\frac{1}{\rho}\left(\frac{\partial}{\partial x_1^2}+\frac{\partial}{\partial x_3^2}+\frac{\omega^2}{c_l^2}\right).$$

The Green's function, $G(x_1,x_3;x_1',x_3'|\omega)$ is the solution of an equation similar to Eq. (3), namely

$$\frac{1}{\rho}\left(\frac{\partial^2}{\partial x_1^2}+\frac{\partial^2}{\partial x_3^2}+\frac{\omega^2}{c_l^2}\right)G(x_1,x_3;x_1',x_3'|\omega)=\delta(x_1-x_1')\,\delta(x_3-x_3'), \tag{4}$$

with appropriate boundary conditions. Solutions of Eq. (4) are known in the following two cases: an unbounded fluid and a fluid bounded by a planar rigid surface.[8] The Green's function, G^∞, of an infinite unbounded fluid is given by

$$G^\infty(x_1,x_3;x_1',x_3'|\omega)=-\frac{i\rho}{4}H_0^{(1)}\left\{\frac{\omega}{c_l}[(x_1-x_1')^2+(x_3-x_3')^2]^{1/2}\right\}, \tag{5}$$

where $H_0^{(1)}$ is a Hankel function of the first kind. The Green's function, g_b, for the semi-infinite fluid bounded by a rigid planar surface $x_3=0$, is also known and takes the form

$$g_b(x_1,x_3;x_1',x_3'|\omega)=-\frac{i\rho}{4}\left[H_0^{(1)}\left\{\frac{\omega}{c_l}[(x_1-x_1')^2+(x_3-x_3')^2]^{1/2}\right\}+H_0^{(1)}\left\{\frac{\omega}{c_l}[(x_1-x_1')^2+(x_3+x_3')^2]^{1/2}\right\}\right]. \tag{6}$$

The Green's function for the fluid in contact with a rigid planar solid supporting a raised feature is not known analytically but it can be constructed mathematically by cutting out of the semi-infinite fluid the volume occupied by the defect a (Fig. 1). This mathematical operation is achieved by the application of a cleavage operator V onto g_b. The cleavage operator is defined as $(1/\rho)(\partial/\partial n)$, where $\partial/\partial n$ means the normal derivative at the boundaries.[9] The cleavage operator is therefore only defined in the space M of the interface being cut. Here M represents the surface of the raised feature. We obtain the Green's function, g_f, of the fluid in which one has made a cut corresponding to the surface of the linear defect from

$$g_f(M,M)[I(M,M)+V(M,M)g_b(M,M)]=g_b(M,M), \tag{7}$$

where $I(MM)$ is the unit matrix. In Eq. (7) we have used the notation (M,M) for $((x_1,x_3)\in M,(x_1',x_3')\in M)$. Equation (7) is an integral equation, with integration over the solid/fluid interface space M. Once the interface elements of g_f are known in the space M from Eq. (7), we can deduce the Green's function in the space D encompassing the entire fluid through

$$g_f(D,D)=g_b(D,D)+g_b(D,M)[g_b^{-1}(M,M)g_f(M,M)-\mathrm{I}(M,M)]g_b^{-1}(M,M)g_b(M,D). \tag{8}$$

The first term in the right-hand side of Eq. (8) is the Green's function of the fluid bounded by a planar interface. The second term represents a correction to the Green's function of the fluid with a planar interface that accounts for the presence of a raised linear feature. This term arises from scattering of acoustic waves by the linear defect.

We can therefore define a scattering function $T_b(MM)$

$$T_b(M,M)=[g_b^{-1}(M,M)g_f(M,M)-\mathrm{I}(M,M)]g_b^{-1}(M,M) \tag{9}$$

such that Eq. (8) becomes

$$g_f(D,D)=g_b(D,D)+g_b(D,M)T_b(M,M)g_b(M,D). \tag{10}$$

Equation (10) is sufficient to solve the problem of scattering of an acoustic wave by the defect a. We denote by $|\Phi(D)\rangle$, the pressure field for a wave in the semi-infinite fluid bounded by a planar surface, that is, the pressure field associated with the Green's function g_b. Then, by analogy with Eq. (10), the pressure field, $|\phi(D)\rangle$ in the fluid bounded by a surface supporting a linear feature can be written in the form

$$|\phi(D)\rangle=|\Phi(D)\rangle+g_b(D,M)T_b(M,M)|\Phi(M)\rangle. \tag{11a}$$

Equation (11a) can be written formally as

$$|\phi(D)\rangle=|\Phi(D)\rangle+|\phi^{(s)}(D)\rangle, \tag{11b}$$

where the second term is the wave scattered by the raised feature.

From a practical point of view, let us consider the case of an incident compression wave of frequency, ω, travelling towards the surface with an incident angle θ_i. Then

$$\phi^{(i)}(x_1x_3|\omega)=\frac{W}{2}\exp\left[\frac{i\omega}{c_l}(x_1\sin\theta_i-x_3\cos\theta_i)\right], \tag{12}$$

where $W/2$ is the amplitude of the pressure wave. Because the acoustic wave is reflected by the rigid planar surface, the pressure field $|\Phi(D)\rangle$ in the semi-infinite liquid takes the following representation:

$$\Phi(x_1x_3|\omega)=\frac{W}{2}\left\{\exp\left[\frac{i\omega}{c_l}(x_1\sin\theta_i-x_3\cos\theta_i)\right]+\exp\left[\frac{i\omega}{c_l}(x_1\sin\theta_i+x_3\cos\theta_i)\right]\right\}, \tag{13}$$

where the second term gives the reflected compression wave from the perfect planar surface. Equation (13), therefore, gives the acoustic wave associated with the Green's function g_b of Eq. (6). In the presence of linear defect a on the solid surface, the total pressure field is given by Eq. (11). Therefore, provided we can calculate the scattering function, we shall be able to calculate the total field $\phi(x_1,x_3|\omega)$ at any observation point (x_1,x_3) in the fluid (which means both near and far field).

In order to obtain the scattering function and the pressure field, one solves numerically the integral Eqs. (7), (9), and (11). For this, we discretize space which transforms these equations into discrete matrix relations. For this purpose, the axis x_1 is divided into $2N$ intervals having their middle at the points $\{x_n\}$ such that

$$x_n=(n+1/2)\Delta x$$

with $n=-N,-N+1,...,N-1$; and $\Delta x=R/N$.

In this way, the continuous curve delimiting the interfacial space M is divided into small segments. In practice N is chosen to be $N=200$ in order to have a good balance between convergence and computation time. The matrix $g_f(M,M)$ is then calculated from known matrices using Eq. (7). It is then inserted into Eq. (9) to obtain the scattering matrix, $T_b(MM)$, which in turns is used into Eq. (11a) to determine the pressure field in the fluid. Further details of the calculation as well as the numerical procedure are given in Refs. 10 and 11.

We shall be more particularly interested in evaluating the total pressure on the surface of the defect (space M). Indeed, the knowledge of $\phi(MM)$ will enable us to obtain the total acoustic force acting on the defect by summing the pressure over the contour of the defect

$$\boldsymbol{F}=\int \phi\mathbf{n}\cdot ds. \tag{14}$$

ds is an element of length along the contour of the defect cross section. With this definition, the force $\boldsymbol{F}$ is given per unit length along the defect, that is, along x_2. This force is decomposed into two components, namely a component normal to the substrate F_n and a tangential component F_t parallel to the direction x_1.

We report in Figs. 3 and 4, the numerical results of our calculations for the normal and tangent components of the force on the defect as a function of frequency and angle of incidence. In these figures, the components of the acoustic force and the frequency are normalized by the quantity WR and R/c_l, respectively. The normalized component of the force perpendicular to the wafer surface approaches the asymptotic value of 1 as the reduced frequency decreases to zero. In this limit the force experienced by the raised feature is simply due to a difference in uniform static pressure between the solid and the fluid. For that reason the asymptotic value is independent of the incidence angle. In this same limit, the near uniformity of the pressure field around the defect leads to the vanishing of the tangent component of the force. As frequency increases, the pressure field around the defect is not uniform anymore. Different points along the surface of the defect feel different pressures leading to an increase in the tangent force and a decrease in the normal force. Moreover, with larger frequencies and smaller wavelength, it is clear from the force oscillations that scattering of the incident wave by the defect becomes more important.

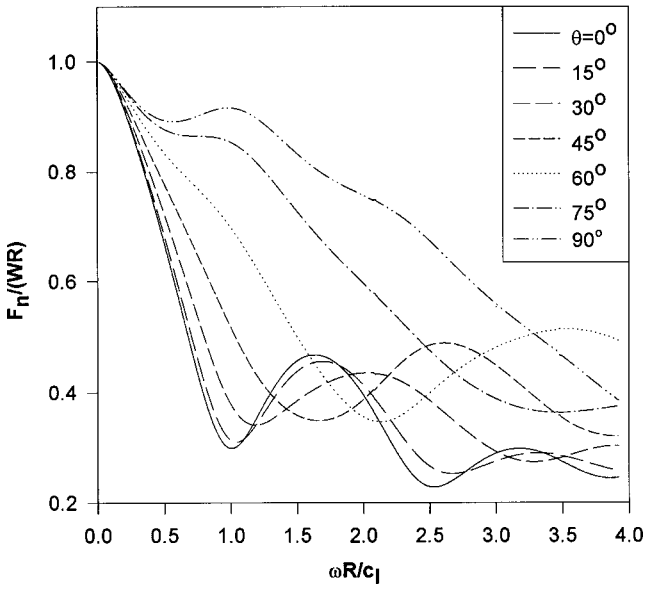

FIG. 3. Variation of the amplitude of the normal force (in units of WR) along the defect surface (space M) as a function of the reduced frequency ($\omega R/c_l$) for different values of the incident angle. The liquid region is composed of water.

Moreover, at short wavelength (i.e., larger frequencies), scattering makes the effect of the incidence angle more significant. We note, however, that in megasonic cleaning of silicon features on a silicon substrate the reduced frequency remains very small. For instance in the case of a raised feature composed of silicon with a width of 1 μm ($R=0.5$ μm) and an incident wave of 1 MHz in water, the reduced frequency, $\omega R/c_l$ amounts to 2.1×10^{-3}. Even for larger size features up to $R\sim125$ μm constituted of softer materials than silicon such as metallic wires (see Table I), the reduced frequency does not exceed 0.5. This indicates that scattering

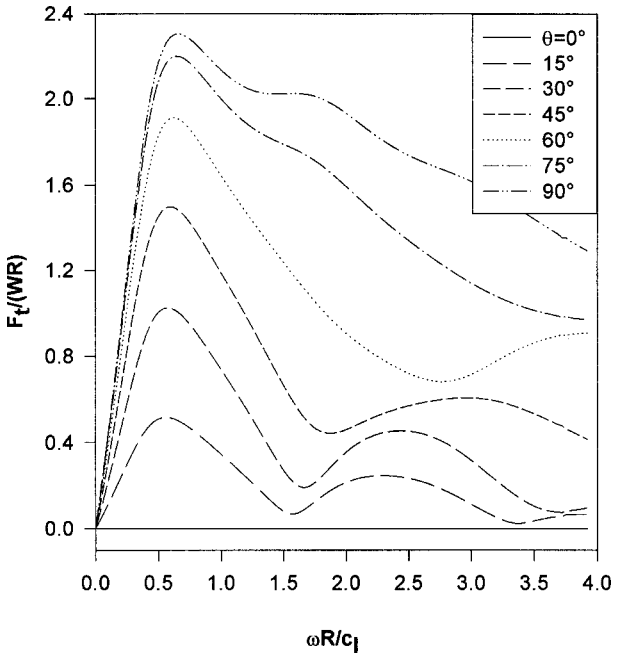

FIG. 4. Same as in Fig. 3 for the tangential force amplitude.

TABLE I. Longitudinal and transverse speeds of sound for selected materials (after Ref. 18).

Material	c_l (m/s)	c_t (m/s)
Silicon	8433	5843
Aluminum	6420	3040
Copper	5010	2270
Gold	3240	1200
Water	1500	···

of the incident megasonic wave by most linear defects that may be encountered in practical situations is negligible. In this case, the main contribution to the normal force arises from the pressure difference between the solid and the fluid, and is nearly independent of the incidence angle and frequency. The reduced normal force, F_n/WR, is then nearly equal to 1. In contrast, the tangential component of the reduced force depends strongly on frequency and incidence angle in the practical range of frequencies employed with megasonic cleaning. For a reduced frequency in the interval [0,0.5], the reduced tangential force can be approximated by a linear relationship of the form

$$\frac{F_t}{WR}=\alpha\frac{\omega R}{c_l},$$

with $\alpha=4.3587\sin(1.0538\theta-5.3733)+0.040\,97$, where θ is in degrees.

Since the tangential force F_t is calculated per unit length of defect, the total tangential acoustic force on the defect is then proportional to its volume. This force results then from the pressure gradient across the defect due to the passing acoustic wave.[12] As the wavelength shortens, the pressure gradient increases and so does the tangential force. Of course, beyond a certain frequency (corresponding to a reduced frequency exceeding 0.5), well above the value corresponding to experimental conditions, scattering will become important and the simple linear form for the reduced tangential force is not valid anymore.

III. APPLICATIONS

We consider the application of the previous calculations to two types of raised linear features with significantly different sizes that may be encountered in megasonic cleaning of open-package integrated circuits. The first feature is a micron-size silicon ridge on the silicon substrate while the second one consists of a metallic wire bonded on a silicon wafer with a diameter in the tens to hundreds of microns.

A. Raised silicon feature on silicon substrate

We may now calculate the stress exerted on a raised silicon linear feature by the acoustic wave. At megasonic frequencies, the normal force is due to the pressure difference between the solid and the fluid. Therefore, the substrate is subjected to the same normal force as that of the defect, resulting in a zero net normal force on the defect. The tangential force, however, leads to a shear stress whose magnitude may be estimated by $\tau=F_t/2R$. In obtaining this ex-

pression we recall that F_t is already expressed per unit length of defect and that the width of the defect at its base is $2R$.

In a megasonic cleaning tank, the pressure amplitude $W/2$ is nearly 4 atm (or 4×10^5 Pa) for a transducer operating at 250 W.[13] This would result in the shear stress $\tau = 0.004$ MPa at an incidence angle $\theta = 90°$ for which the normalized tangent force is $F_t/WR \sim 0.01$. Under the condition that the raised feature is constituted of silicon, megasonic cleaning may damage the patterned wafer if the acoustic shear stress exceeds the shear strength of silicon. Let us now estimate the shear strength of silicon. The theoretical tensile strength of a brittle material may be estimated by the relation[14] $\sigma_{\text{th}} = (\gamma E/a_0)^{1/2}$ where γ is the surface tension, E is Young's modulus, and a_0 is the interatomic spacing. The interatomic distance between silicon atoms is $a_o = 2.3517$ Å. Young's modulus E varies with the silicon crystallographic orientation and takes the values of 13×10^{10}, 17×10^{10}, and 19×10^{10} Pa for the orientations [100], [110], and [111]. The surface energy of silicon also depends on the crystallographic orientation of the surface and takes the values 1.23, 1.51, and 2.13 J/m^2 for the orientation [111], [110], and [100], respectively. We can therefore estimate a range for the theoretical strength of 31.5–34.3 Gpa. The theoretical strength typically overestimates the strength of the materials and the experimental strength is approximately 2–3 orders of magnitude lower than the theoretical strength. For instance, the modulus of rupture in bending for silicon varies between 68 and 343 MPa.[15] It is difficult to measure the shear strength of a material but a useful and conservative relationship gives the shear strength $\sim 40\%$ of the tensile strength.[16] With this relation, we estimate the shear strength of silicon to exceed a few tens of megapascals. This value is orders of magnitude larger than the calculated acoustic shear stress under the operating conditions of megasonic cleaning. On another hand, we shall recall that the acoustic force acting on the pattern, and therefore the shear stress, are oscillatory with a frequency on the order 1 MHz. The pattern subjected to a cyclic load may then yield due to fatigue. We estimate the dynamic fatigue strength of silicon to be approximately 50% of its static strength and even that still exceeds the acoustic stress by orders of magnitude. These results, therefore, suggest that the acoustic pressure gives rise to a negligible contribution to the damage of patterned silicon wafers.

B. Wire bonded on wafer

Metallic wires bonded on a wafer constitute another example of raised linear features. Contrary to the previous example where the silicon feature had dimensions very much smaller than the megasonic wavelength, metallic wires have diameters ranging from 25 to 250 μm.[17] The longitudinal and transverse speed of sound in metals such as aluminum, gold, or copper are typically smaller than that in silicon but still significantly larger than that of water (see Table I). Metallic wires bonded on silicon substrates are still, therefore, within the limits of validity of the model developed in Sec. II. Considering the case of gold wires with $R \in [12.5,125]$ μm, the reduced frequency varies between 0.05 for the thinner wire and 0.5 for the wire with the larger diameter. Following the procedure used in the case of the silicon feature, we can calculate the shear stress on a gold wire produced by acoustic force. This stress amounts to approximately 0.088 MPa for a 25 μm diameter wire and 0.88 MPa for a 250 μm diameter wire. Experimental shear strength of gold wires can be estimated from measured shear force data versus bonded area diameter obtained with the ball shear test.[17] This test consists of applying an increasing shear force on a bonded ball until sliding occurs. In ball shear experiments the bond strength is often recorded in gram force and maximum values for aluminum and copper wires amount to approximately 40 g force for 75–90 μm diameter balls.[17] The maximum shear stress for bonded wires can then be estimated to vary in the range 15–25 MPa, which are values well in excess of the acoustic shear stress. However, these shear strengths are maximum values and poorly bonded wires may exhibit significantly weaker bond strength. Only in the extreme case of a very weak bond would megasonic cleaning be susceptible to damaging the wire.

IV. CONCLUSIONS

The interaction between an incident megasonic wave propagating in a fluid and a raised linear defect on a substrate is investigated with a theoretical model based on Green's functions. The fluid is assumed to be nonviscous and to have the acoustic properties of water. The solid substrate and the defect are taken to be rigid. The model provides quantitative information concerning the pressure distribution of the surface of the defect. The pressure field around the defect is integrated over the defect surface to calculate an acoustic force. The acoustic shear stress resulting from the component of the force on the defect parallel to the substrate is then calculated in two cases. The first case considered is that of a micron-size raised linear ridge of silicon on a silicon substrate and the second case consists of a metallic wire with a diameter in the tens of micrometers bonded on a silicon substrate. In both cases the model shows that the acoustic shear stress is not large enough to cause damage to the linear feature. We conclude from the previous results that it is very unlikely that megasonic cleaning may damage patterned wafers in the absence of any other mechanism such as microcavitation or acoustic streaming. Indeed, damage is expected to result from processes that are associated with high energy densities. The scattering of an incident acoustic wave by the raised linear features studied here does not lead to a sufficient energy concentration. In contrast, for instance, during cavitation the formation of a cavity and its subsequent collapse is able to concentrate the low energy density of the sound wave into a very small volume leading locally to very high pressures and temperatures that can erode solids. On the other hand, acoustic streaming may also concentrate energy in small volumes as in thin boundary layers near solid/fluid interfaces (in the case of Schlicting streaming) or near oscillating bubbles (in the case of microstreaming). An extension of the present work that includes acoustic streaming is underway and will be the subject of another publication.[19]

[1] S. Schwatzman, A. Mayer, and W. Kern, RCA Rev. **46**, 81 (1985).
[2] R. Gouk, M. S. thesis, University of Minnesota, 1996.

[3] C. Eckart, Phys. Rev. **73**, 68 (1948).
[4] H. Schlicting, *Boundary-Layer Theory*, 6th ed. (McGraw-Hill, New York, 1968).
[5] S. A. Elder, J. Acoust. Soc. Am. **31**, 56 (1959).
[6] W. G. Mayer, J. Appl. Phys. **34**, 909 (1963).
[7] K. Ergin, Bull. Seismol. Soc. Am. **42**, 349 (1952).
[8] P. M. Morse and H. Feshbach, *Methods of Theoretical Physics* (McGraw-Hill, New York, 1953).
[9] L. Dobrzynski, Surf. Sci. Rep. **11**, 139 (1990).
[10] B. Djafari-Rouhani and L. Dobrzynski, J. Phys.: Condens. Matter **5**, 8177 (1993).
[11] A. Kheif and B. Djafari-Rouhani, J. Appl. Phys. **81**, 7141 (1997).
[12] M. Olim, J. Electrochem. Soc. **144**, 3657 (1997).
[13] D. Zhang, Ph.D. dissertation, University of Minnesota, 1993.
[14] W. D. Kingery, H. K. Bowen, and D. R. Uhlmann, *Introduction to Ceramics*, 2nd ed. (Wiley, New York, 1976).
[15] F. Shimura, *Semiconductor Silicon Crystal Technology*, (Academic, New York, 1989).
[16] K. G. Budinski, *Engineering Materials*, 4th ed. (Prentice-Hall, London, 1992).
[17] G. G. Harman, *Reliability and Yield problems of Wire Bonding in Microelectronics*, International Society for Hybrid Microelectronics (McGraw-Hill, New York, 1993).
[18] D. R. Lide, *Handbook of Chemistry and Physics*, 71st ed. (CRC, Cleveland, OH, 1990).
[19] P. A. Deymier, J. O. Vasseur, A. Khelif, B. Djafari-Rouhani, L. Dobrzynski, and S. Raghavan (unpublished).